Performance analysis of PV and Wind Stand Alone hybrid energy systems

[1]Sakku C. M., [2]Ramesh L. Chakrasali
[1]Department of Electronics & Communication Engineering
Jain College of Engineering & Technology, Hubli
[2]Department of Electrical & Electronics Engineering
SDM College of Engineering and Technology, Dharwad

***Abstract*:**

Hybrid renewable energy systems are in trend nowadays. Pairing two complementary energy forms has proven to be sustainable. It is evident from the literature that wind and photovoltaic systems are recommended for hybrid energy systems, as they complement each other in their energy pattern. Also, the wind PV hybrid system leads to an enhanced system efficiency and improved stability to a certain degree. The system is even though sustainable, a challenge in itself in bringing two different cadres of power to work as a single unit requires a power electronics converter and inverter design. In this paper, an attempt is made to generate power using stand-alone systems constituting wind and photovoltaic systems for household applications. An effort is made to simulate the PV and wind hybrid system, wherein the output is connected to a common DC bus, which is further inverter to supply power to the user end. The whole system is simulated under a MATLAB environment, and a study is made to analyze the performance of this hybrid PV and Wind energy system for different load patterns from the user end. The whole system is simulated under a MATLAB environment, and a study is made to analyze the performance of this hybrid PV and Wind energy system for different load patterns from the user end.

Keywords: *Hybrid Renewable Energy Systems, DC bus, Photovoltaic systems, Wind Energy Systems, Permanent Magnet Synchronous Generators (PMSG)*

1. INTRODUCTION

Hybrid Renewable Energy Systems (HRES) are considered as one of efficient energy systems. Combining two or more energy forms to compel maximum energy is in huge demand. Also, when two energy systems which are complimentary to each other are combined, the system is enhanced. According to the Ministry of Power in India, a lot of scope is given to strengthen the use of renewable energy systems. As India is in the equatorial region photovoltaic and wind energy systems are available all through the year with a tolerable climatic variation. Also, due to technical advances, there is huge growth in this sector which is depicted in Figs 1,2 and 3 below.

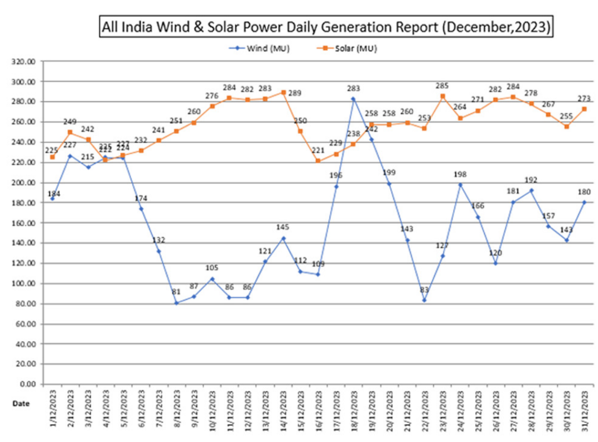

Fig 1: Daily solar and wind power generation trend in December -2023

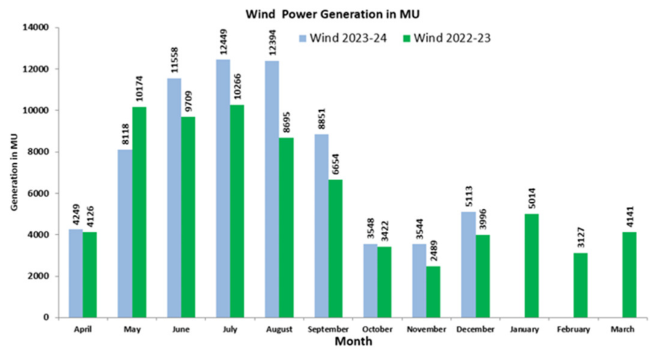

Fig 2: Month Wise Wind Power Generation for the year 2022-23 and year 2023-24

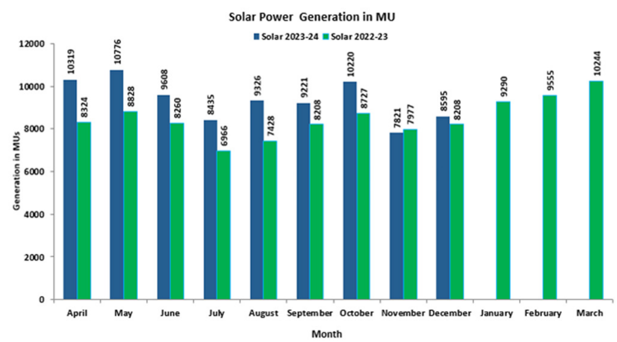

Fig 3: Monthly Wise Solar Power Generation for the year 2022-23 and year 2023-24.

Fig 1,2 and 3 show the month-wise wind and photovoltaic system power generation. It also validates that for a geographically centered location like India, the is a huge scope for wind and photovoltaic hybrid systems. Solar and wind power is naturally intermittent and can create technical challenges to the grid power supply especially when the amount of solar and wind power integration increases or the grid is not strong enough to handle rapid changes in generation levels. In addition, if solar or wind are used to supply power to a stand-alone system, an energy storage system becomes essential to guarantee a continuous supply of power. The size of the energy storage depends on the intermittency level of the solar or wind [21].

In the proposed system, an attempt is made to integrate two energy systems namely, the Photovoltaic system and wind energy system. To model a Photovoltaic system, a single diode model is used, as the model provides near approximate values of voltage and current at a given irradiance in comparison with the manufacturer's datasheet. The same is simulated in the MATLAB environment for a power rating of 2.5KW [1]. The wind system is modelled using a 2-mass drive train model, fed by a 3Φ Permanent Magnet Synchronous Generator (PMSG) with pitch angle control. The same is simulated under MATLAB environment for a rating of 5KW.

The paper has been sub-divided as follows:

1. The *Introduction* section provides a bird view of the overall system.
2. The *Overall System design* section provides the details of the PV and wind system ingredients
3. In the *Methodology* section, a detailed view of the individual system and its simulated values has been discussed.
4. The *Hybrid (Photovoltaic + Wind) Energy model* section elaborates the simulation of integrated wind and PV models under MATLAB environment
5. The *Results and Discussion* section provides a numerical analysis of variation voltage and current for different load patterns.
6. The *Conclusion* section draws the conclusions derived based on results and discussion.

2. THE OVERALL SYSTEM DESIGN:

The wind and PV systems are combined and connected to a common DC bus. A block diagram in Fig 4 provides a brief picture of the system design. Designing renewable energy hybrid systems involves sizing and selecting the best components to provide affordable, efficient and effective renewable energy. A grid-connected SWHS's performance was examined, but when wind speed increased, the blade pitch angle control (BPAC) was not used to limit output wind power[17]. The study conducted in [18,19] focused solely on wind energy and did not take into account any other renewable energy sources. limit wind power output when the wind speed is higher

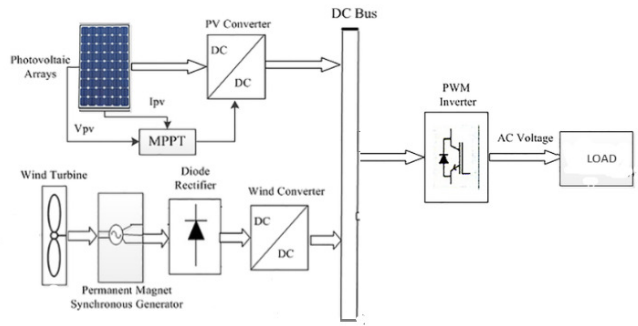

Fig 4: Overall Block diagram

Fig 4 shows a block diagram of the overall system. It contains a photovoltaic system, which is modelled as a single diode model providing an output power of 2.350KW and wind energy systems, with the wind turbine connected to a Permanent Magnet Synchronous Generator (PMSG) through a 2-mass drive train, delivering a 3-phase ac power of 4.230KW. To increase the PV system efficiency, a Maximum Power Point Tracking (MPPT) algorithm has been included in the photovoltaic system. Since the system deals with voltage control, a conventional P&O algorithm has been included. On the other hand, in the wind energy system, a pitch angle controller has been included, which perturbs the variation in the wind speed to a nominal value. The autonomous power system, also known as a stand-alone system, is a great option for isolated locations where utility facilities, especially transmission lines, are expensive to operate or challenging to establish because of their complex nature or other factors. One might further categorise the stand-alone systems into common DC buses and common AC buses. By integrating the two resources into an ideal combination, the fluctuating nature of solar and wind resources can be somewhat mitigated, increasing the system's reliability. For a while, the advantages of one source could outweigh the disadvantages of the other[22-24].

The wind system connected to a PMSG produces a 3-phase power output. This is further connected to a 3-phase bridge rectifier (Universal bridge) to convert the output in terms of DC power. Thus, the wind energy system is designed to produce a DC as output power. On the other hand, in a photovoltaic system, the out-of-PV panel, modelled as a single diode model is connected to an MPPT tracker, producing modulated duty cycles, which is fed as an input to the gating pulse of the switch in the boost converter, producing DC power output. These two systems, PV + Wind together connected to a common DC bus. This system is connected to a common DC bus, using a 3-phase bridge converter to the wind energy system and boosting the PV system voltage using a boost converter. Thus, the system delivers a DC power output. To match the voltage of both systems, a potential divider is used in the PV system. A DC to single phase inverter is used to feed the user end to meet their energy demand.

The major constituents of the overall system are:

1. Wind energy system: modelled as a 2-mass drive train model
2. Photovoltaic system: modelled as a single diode model
3. A common DC bus
4. Inverter at the user end

1) The constituents of wind systems are as in Fig 5 below:
   - i) A wind turbine of 5KW rating: directly derives from the SIMULINK toolkit
   - ii) A PMSG connected to the turbine: Specification- 20Nm, 300V_{DC} and 2200rpm
   - iii) A 2-mass drive train model: an interference between turbine and generator
   - iv) Pitch angle control
   - v) A universal bridge: to convert 3Φ ac power to DC power.

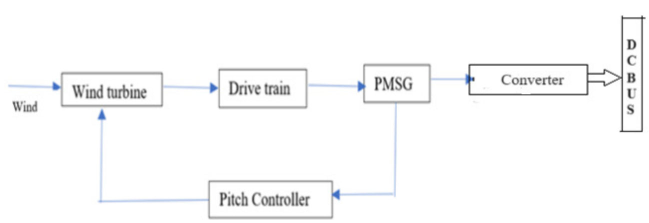

Fig 5: Block diagram of a Wind module

Fig 5 provides a brief description of the wind system configuration

2) The constituents of photovoltaic systems are shown in Fig 6 below [3]. The details are as below:
   i) A combined system (series and parallel combination) of solar panels to deliver a power of 2.350KW
   ii) An MPPT algorithm: A conventional Perturb & Observe method to maintain the knee voltage
   iii) A boost converter: The DC-DC boost converter using IGBT is designed to arrive at the desired voltage level.

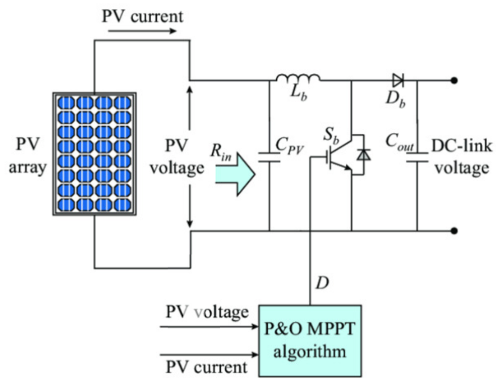

Fig 6: Block diagram of a PV module

Fig 6 provides a brief description of the PV system configuration

iv). A common DC bus: The DC bus voltage is a common platform wherein both systems are combined. The DC bus is maintained at a constant voltage of 90V. However, before connecting PV and wind systems, both the system voltages are made similar.
v). Inverter at the user end: The DC bus voltage is converted to the required AC voltage level by using a power electronic converter. The voltage is converter to a 230V, 50Hz AC voltage.

3. METHODOLOGY:

The mathematical simulation of the system is carried out in a MATLAB environment. In the current section, an attempt is made to revive the individual system along with its components, in detail.

3.1 THE WIND ENERGY MODEL:

The input for the wind systems is the wind speed. The wind system is designed for a wind speed of 12m/s as discussed below[19].

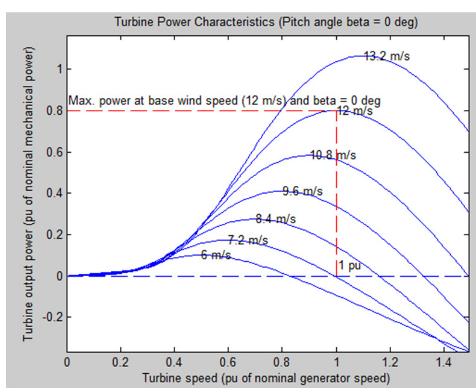

Fig 7: Power output of Wind turbine vs. turbine speed

Fig 7 shows the variation in the turbine torque for variation in wind speed. The model uses a variable-speed wind turbine, which has a base speed of 12 m/s and details are mentioned in Table 1[11]

Table 1: Wind turbine parameters

Parameters	Value
Nominal mechanical output Power (KW)	5
The base power of the electrical generator (VA)	4.5
Base wind speed (m/s)	12
Maximum power at base wind speed (pu of nominal mechanical power)	0.8
Base rotational speed (pu of generator)	1

The model is based on the steady-state power characteristics of the turbine. The stiffness of the drive train is infinite and the friction factor and the inertia of the turbine must be combined with those of the generator coupled to the turbine. The output power developed by the turbine is given by equation 1 [2].

3.1.1 TWO-MASS DRIVE TRAIN MODEL:

A wind turbine's drive train is its mechanical system, which consists of a gearbox, generator, and turbine. The turbine and generator are primarily responsible for this system's inertia. Only a small portion is contributed by the gearbox's teeth wheels [3]. As a result, the gear's inertia is occasionally disregarded, and only the gear system's transformation ratio is considered. Nonetheless, the gear ratio is taken to be unity in this scenario. As a result, the drive train is represented as a two-mass model that includes a connecting shaft and all of the inertia and shaft parts [2]. The wind turbine's low speed is transformed into the necessary generator turbine speed by a gearbox. The drive train model in power systems simulations is often represented by two masses: the generator rotor (high-speed shaft) and the wind turbine rotor (blades, hub, and low-speed shaft) are represented by the first mass. A lumped model of the two-mass drive train is presented in Fig 2.3. It includes turbine inertia J_T (N m s^2/rad), generator inertia J_G (Nms^2/rad), turbine friction damping D_T (Nms/rad), generator friction damping D_G (N m s/rad), and shaft stiffness K_{sh} (Nm/rad)[4]. This lumped model is simple, and it is considered a more exact simulation model. The governing equations of a drive train model are:

$$2Ht + \frac{d\omega t}{dt} = Tm - Ts \quad \text{………………(1)}$$

$$\frac{1}{\omega(ebs)}\frac{d\theta(sta)}{dt} = \omega t - \omega r \quad \text{……………….(2)}$$

$$Ts = Kss^{*}\,\theta sta + Dt\frac{d\theta(sta)}{dt} \quad \text{………..(3)}$$

where,
Ht – inertia constant of the turbine (Nms^2/rad)
θ_{sta} – shaft twist angle (rad)
ω_t – angular speed of turbine (rad/s)
ω_r – rotor speed of generator (rad/s)
ω_{ebs} – electrical base speed (pu)
T_s – shaft torque (Nm)
K_{ss} – shaft stiffness (Nm/rad)
D_t – damping co-efficient (Nms/rad)

The dynamic equations are obtained from Newton's equations of motion for each mass (rotational speed) and shaft (torsion or twist angle). where ω_t and ω_r [per unit (p.u.)] are the turbine and generator speeds, respectively; θ_{sta} [rad] is the shaft twist angle; H_t and H_g are the turbine and generator inertias, respectively; ω_{els} [rad/s] is the electrical base speed; Pt [p.u.] is the turbine input power (here assumed as constant); and T_s and T_e [p.u.] are the shaft and generator torques, respectively [3]

Fig 8 provides the details of a 2-mass drive train modelled in Matlab/Simulink. Table 3 provides the complete parameter details used in the modelling.

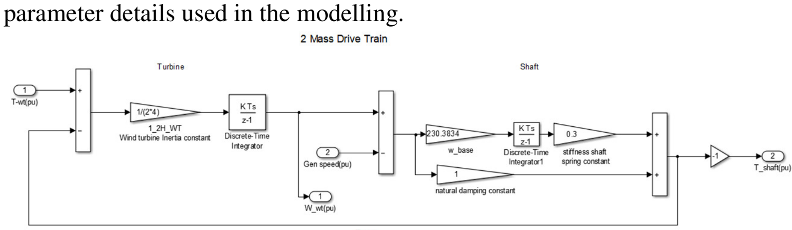

Fig 8: 2-mass drive train model in SIMULINK environment

Table 2: Drive train parameters

Parameters	Value
H_t ; H_g	4s ; 0.1Ht
K_{ss}	0.3 pu/el.rad
D_t	1 pu/el.rad

3.1.2 PERMANENT MAGNET SYNCHRONOUS GENERATOR

An electrical device that transforms the mechanical input from the wind turbine into electrical energy is called a permanent magnet synchronous generator. A PMSG's equations are represented in the d-q frame, which is the rotor reference frame. The stator is the reference point for all quantities in the rotor reference frame. With the well-known benefits of a straightforward rotor design devoid of field windings, slip rings, and excitation systems, a permanent magnet has been widely employed to replace the excitation winding in synchronous machines[13]. Consequently, there will be no heat dissipation in the rotor winding, increasing overall efficiency. The PMSG has garnered significant attention in the WECS field recently because of its small size, increased power density, lower losses, high dependability, and durability. The following equations can be used to represent the PMSG dynamic model in a rotating reference frame.

$$V_q = - R_s i_q - L_q \frac{diq}{dt} - \omega_r L_d i_d - \omega_r \lambda_{m0} \qquad \text{…………(4)}$$

$$V_d = - R_s i_d - L_d \frac{did}{dt} - \omega_r L_q i_q \qquad \text{…………(5)}$$

The expression for electromagnetic torque in the rotor can be written as

$$Te = \left(\frac{3}{2}\right)\left(\frac{P}{2}\right)\left[(L_d - L_q)\, i_q\, i_d - \lambda_m i_q\right] \qquad \text{…………(6)}$$

In the case of a cylindrical rotor, the Ld≈Lq and hence the above equation reduces to

$$Te = \left(\frac{3}{2}\right)\left(\frac{P}{2}\right)\lambda_m i_q \qquad \text{…………(7)}$$

where,

Lq, Ld - q and d axis inductances (H)
R - Resistance of the stator (Ω)
iq, id - q and d axis currents(A)
V_q, V_d - q and d axis voltages (V)
ω_r - Angular velocity of the rotor (rad)
λ - Amplitude of the flux induced by the permanent magnets of the rotor in the stator phases (web)
p - Number of pole pairs
T_e - Electromagnetic torque

Table 3 provides the details of the PMSG parameters used in the system

Table 3: PMSG parameters

Parameters	Value
Power rating	4610W
No. of phase	3
Rotor type	Salient Pole
Stator per phase resistance Rs	0.129 Ω
Inductance [Ld; Lq]	0.001453 H; 0.001607H
Pole pairs	4
Synchronous speed	2200 rpm

3.1.3 PITCH ANGLE CONTROL

The pitch angle (β) is the angle between the direction of wind to the direction of the turbine blade. The power flow is maximum when this angle is zero. Typically, the pitch angle controller is only triggered by strong winds. Under such conditions, it is no longer possible to regulate the rotor speed by raising the generated power because doing so will overload the converter and/or generator. To restrict the rotor's aerodynamic efficiency, the blade pitch angle is altered. By doing this, the rotor speed is kept from rising too high. The generator's rotor speed will increase if the output and wind energy input are not balanced in terms of power. To achieve a balance between mechanical and electrical power, the pitch angle needs to be adjusted. The pitch angle will return to normal operation following the failure. [5].

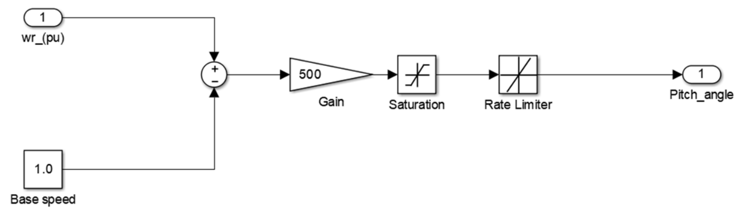

Fig 9: Simulink model of Pitch angle control

The power coefficient CP is significantly influenced by the pitch angle. In traditional generators, it serves as the governor. The pitch control is rarely activated and is set to the ideal setting at low and medium wind speeds. Pitch angle control works to manage the extracted wind power at high wind speeds so that the turbine's design limits are not exceeded [4]. The pitch angle controller is shown in Fig 9.

3.1.4 THREE-PHASE AC TO DC CONVERTER

The 3Φ output power from a PMSG is converted to DC power using a universal bridge. The DC power from the bridge is connected to a common DC bus,

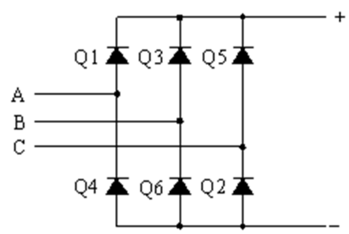

Fig 10: Universal bridge circuitry

As in Fig 10, the Universal Bridge block implements a universal three-phase power converter that consists of six diodes connected in a bridge configuration. The specifications are here below:

Table 4: Universal Bridge Parameter

Parameter	Value
Number of bridge arms	3
Snubber resistance Rs (Ω)	1000
Snubber capacitance Cs (F)	Inf
Power Electronic Device	Diode
Ron (Ω)	1e-3
Lon (H)	0
Forward Voltage V_f(V)	0

Table 4 provides the details of the universal bridge and its value in detail. The Universal Bridge block implements a universal three-phase power converter that consists of up to six power switches connected in a bridge configuration.

3.2. PHOTOVOLTAIC SYSTEM

3.2.1 SINGLE DIODE MODEL

A single-diode model is selected after simulating different models and a single-diode model is found to be closer to the manufacturer's datasheet. Also, the model is very simple and accurate during normal conditions. A current source and a parallel diode can be used to demonstrate an ideal PV cell. The series and shunt resistances are regarded as 0 and infinite, respectively, in the ideal scenario. Nonetheless, it is important to take into account that the series and shunt resistances in a practical system have finite values [9].

The governing equations of a single-diode model are listed below:

Photo Current,

$$\mathrm{Iph} = \mathrm{Isc} + \mathrm{Ki} * (\mathrm{T} - 298) * \frac{\mathrm{G}}{1000} \quad (1)$$

$$\text{Saturation current, } \mathrm{Io} = \mathrm{Irs} * \left(\frac{\mathrm{T}}{\mathrm{Tn}}\right)^3 * \exp\frac{\mathrm{q} * \mathrm{Eg0} * [\left(\frac{1}{\mathrm{Tn}}\right) - \left(\frac{1}{\mathrm{T}}\right)]}{\mathrm{nk}} \quad (2)$$

Reverse Saturation Current,

$$Irs = \frac{Isc}{[e^{\frac{q*Voc}{n*Ns*K*T}}]-1} \qquad (3)$$

Current through the shunt resistor,

$$Ish = \frac{V+(I*Rs)}{Rsh} \qquad (4)$$

Output Current,

$$I = Iph\text{-}Io^{*}\left[e^{\frac{q*(V+I*Rs)}{n*k*Ns*T}}\right] - 1 \qquad (5)$$

where,
ki – Short Circuit current of the PV-cell at a temperature of $25^{O}C$ and irradiance of $1000W/m^2$
T & Tn – Operating and Nominal temperature in Kelvin
Q – Charge of an electron
N – Ideality factor of the diode
K – Boltzmann Constant (J/K)
Ego – Bandgap of semiconductor
Rs & Rsh– Series Resistance & Shunt Resistance

The above equations are simulated under the MATLAB environment using the SIMULINK tool set[1].

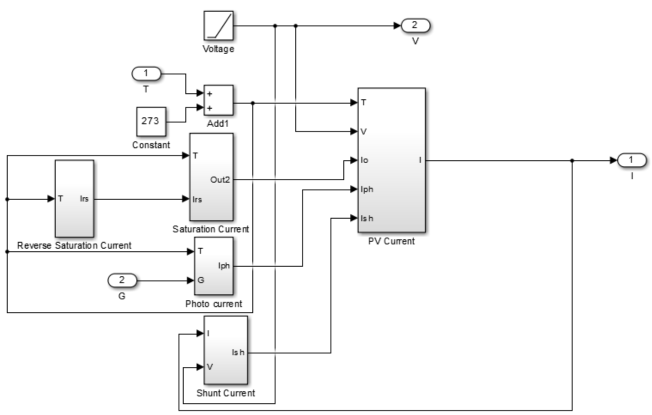

Fig 11: Simulated model of the model

Fig 11 represents the mathematical model connected to represent a photovoltaic system modelled as a single diode model.

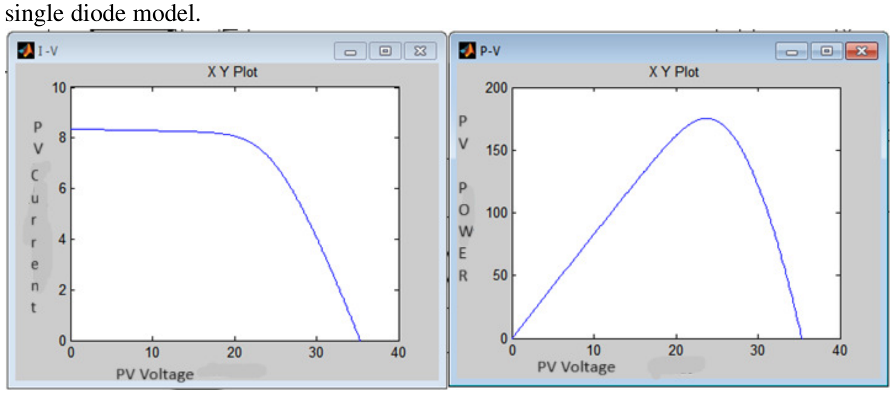

Fig 12: I-V and P-V characteristics of a single PV module

Table 5: Panel Specifications

Parameter	Value
Rated Power (P)	200W
Voltage at maximum power (Vmp)	26.4V
Current at maximum power (Imp)	7.58A
Open circuit Voltage (Voc)	37.40V

Short circuit current (Isc)	8.360A
Number of cells in series (Ns)	54
Number of cells in parallel (Np)	1

3.2.2 FLOW CHART OF MPPT ALGORITHM

The P&O MPPT technique's simplicity, lack of sensor requirements, and minimal control complexity have made it one of the most extensively used methods. A P&O technique is employed to monitor the MPP.[13]. A small disturbance is applied in this method to induce a change in the PV module's power output. The PV output power is then measured regularly and compared to its initial value; if the output power rises, the process is repeated; if not, the perturbation is applied to the PV module or the array voltage. To determine whether the power is increasing or decreasing, the voltage of the PV module is changed. The PV module's operational point is on the left of the MPP when a rise in voltage results in an increase in power [8]. Therefore, to accomplish MPP, more disturbance is needed in the right direction. On the other hand, if a rise in voltage results in a fall in power, this indicates that the PV module's operating point is to the right of the MPP and that additional disturbance to the left is necessary to get to the MPP. Fig. 13 shows the flow chart for the charge controller's chosen P&O algorithm [9]

As illustrated in Fig. 13, the MPPT technique uses the extracted voltage and current from the PV source to power the boost converter. The boost converter's designed components—the inductor Lb, diode Db, capacitor CPV, and switch Sb—provide the necessary voltage level in conjunction with the MPPT controller. [3].

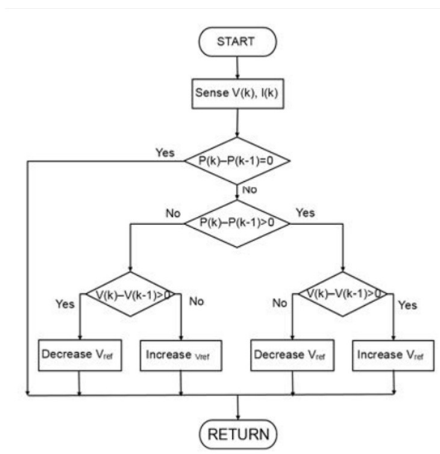

Fig 13: Perturb and Observe (P&O) algorithm used in Photovoltaic modelling

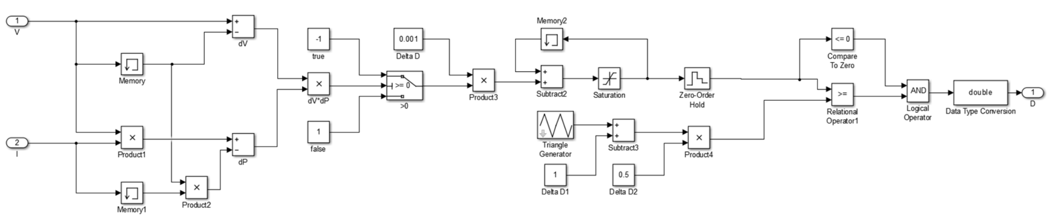

Fig 14: P&O algorithm used in Photovoltaic modelling

3.2.3 BOOST CONVERTER

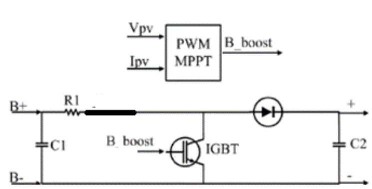

Fig 15: Boost converter using IGBT

Design of a boost converter.
Assumptions and given data:
Vs (Input voltage) = 210V
Output voltage (Vo) = 230V
Output power Po = 5060W (Po=Vo*Io=230V*22V)
Efficiency = 100%
Switching frequency, fsw=25K Hz
Duty cycle, $D = 1 - \frac{Vs}{Vo} * \eta = 0.08695$
$L >= \frac{Vs\ (min) * D}{fsw * \Delta Il}$
where,
ΔIL =20-40%of I_L. 30% of I_L [12],

3.3 THE COMMON DC BUS

As discussed in the above section, the power from the two energy systems is connected to a common DC bus, as the power from both energy systems is inverted to DC power.

Table 6: DC bus parameters

Parameters	Value
Bus Voltage (V)	116.4
Bus Current (A)	5.875
PV voltage (V)	116.4
PV current (A)	3.156
Wind Voltage (V)	116.4
Wind current (A)	2.745

Table 6 provides the details about the bus voltage and bus current, which is further inverted to AC power. To maintain a constant voltage at the bus terminal, a voltage divider circuitry is introduced in the Photovoltaic module at the load end.

3.4 INVERTER

The DC power from the DC bus is now converted to 1Φ, 230V, 50Hz AC power, which is fed to the user for household applications. The inverter from the MATLAB toolkit is utilized. The details of the inverter are as here below:

Table 7: DC bus parameters

Parameter	Value
Number of bridge arms	2
Snubber resistance Rs (Ω)	250
Snubber capacitance Cs (F)	0.1e-6
Power Electronic Device	IGBT/Diode
Ron (Ω)	0.01
Forward voltages (V)	0.7
T_F(s), T_T(s)	1e-6,2e-6

Table 7 provides the detailed specifications of all the parameters configured as inverters.

4. THE HYBRID (WIND AND PV) ENERGY MODEL:

In section 3, a decent discussion on the PV and Wind has been discussed. Section 4 is a focused hybrid model. The unpredictability of wind and solar systems, as well as their reliance on weather and climate change, is a disadvantage. To be fully dependable, both of these (if utilized separately) would need to be bigger, which would increase the overall cost. On the other hand, combining solar and wind energy into a hybrid generating system can lessen their oscillations and boost total energy production [10]. Small-scale hybrid PV–wind systems are complicated to analyse and control. Large systems' size and power range are primarily to blame for this. Analysing the energy management, power conversion, controller performance, etc., is hard work. To get around this problem, though, emulators that mimic the static and dynamic properties of solar and wind power conversion systems have been created [20].

4.1 SIMULATION OF WIND MODEL

Fig 16 shows the simulation of the wind energy model simulated under the MATLAB environment and Fig 17 shows the voltage and current waveform

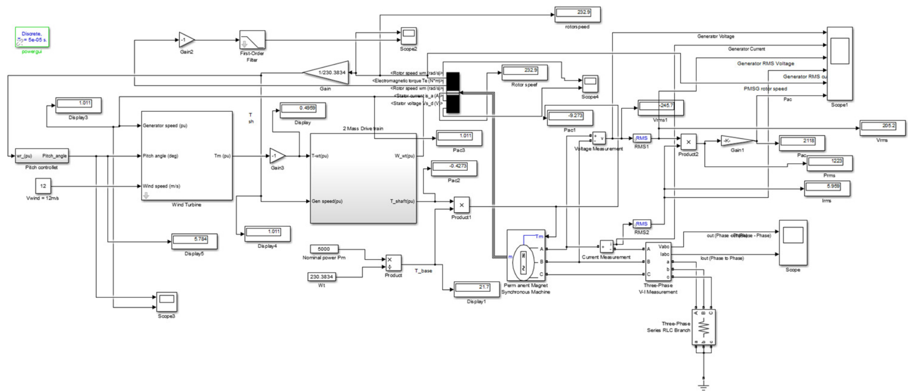

Fig 16: Simulation of Wind system modelled as a two-mass drive train model with pitch angle control using a PMSG

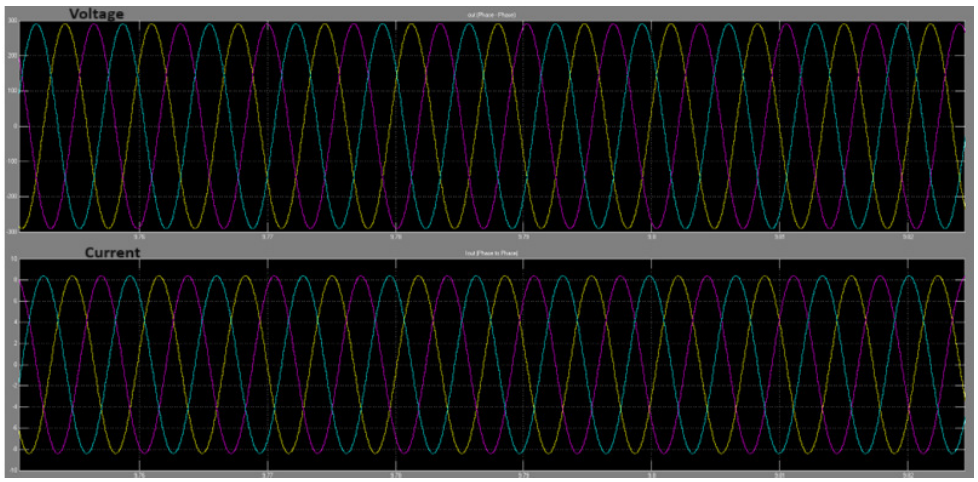

Fig 17: Load voltage and current waveforms of Wind Energy Model

The simulation results of both models are obtained. The output voltage waveforms and the corresponding load currents of the wind model for a speed of 12m/s

Table 8: Voltage and current values at various wind speed

Wind speed (m/s)	Load voltage V_L (V)	Load current I_L (A)	Output power (W)
10	280	8.0	3879.79
11	290	8.4	4219.27
12	292	8.4	4748.37
13	293	8.4	4262.92
14	309	8.9	4736.31

Table 8 provides the details of variations in the voltage and current values in a wind turbine.

4.2 SIMULATION OF PHOTOVOLTAIC MODEL:

Fig 11 represents a single-diode model of a PV cell. The simulation of a single panel along with the I-V and P-V curves have been discussed in section 3 (ref fig 11 and table 5). Fig 18 and Table 9 provide the details of the series and parallel combination of solar panels modelled as a single diode model to achieve the required power rating.

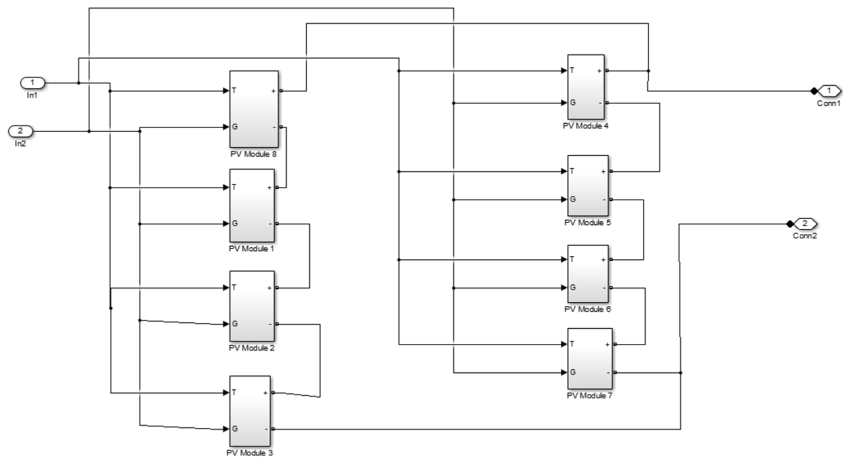

Fig 18: Series and Parallel combination of PV module under MATLAB environment

Table 9: Photovoltaic system configuration

Parameter	Value
The individual output Voltage of each panel	32V
The individual output Current of each panel	8.1A
Number of panels in series	4
Number of panels in shunt	2 strings
PV output Voltage	130.5volts
PV output Current	16amp
Total power developed from a PV system	2150W = 2.15KW

The fig 18 describes that 4 strings are connected in series and a string of two such combinations achieves the required power [1]

4.3 SIMULATION OF HYBRID MODEL

The overall hybrid model is shown in Fig 19. The whole system is simulated in the MATLAB environment to test the suitability of the system.

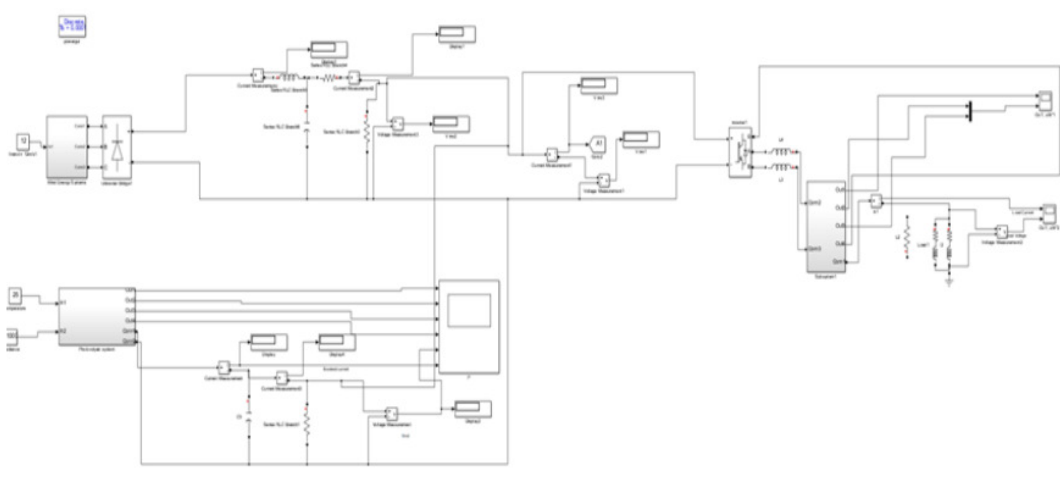

Fig 19: HRES model simulated under MATLAB environment

As in Fig 19 PV and wind hybrid models are depicted. It constitutes both energy systems Photovoltaic systems and wind energy systems. It also shows a boost converter connected to a PV system and a 3Φ bridge rectifier connected to the wind energy system. A common DC bus is present which connects both PV and wind systems system in common. The output of the 3Φ bridge rectifier is further connected to a 1Φ converter to produce a 230V, 50Hz. Ac voltage. A study is made by tabulation voltage and current values for different types of load connected at the output end of the 1Φ converter.

5. RESULTS AND DISCUSSION:

The hybrid model is connected to the load terminal to study the voltage and the current waveforms. The voltage and current waveforms at standard STP conditions at different load combinations are shown in Figs 20,21 and 22 below.

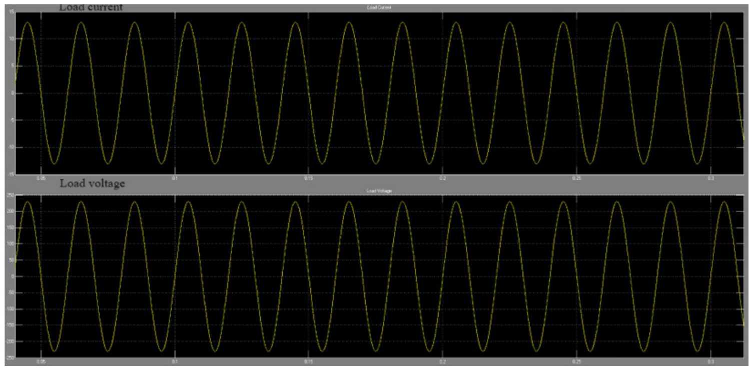

Fig 20: Load voltage and current at 1KW resistive load

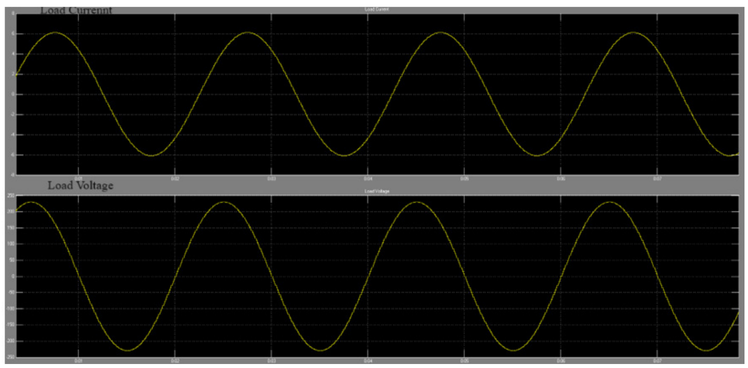

Fig 21: Load voltage and current at 2KVA load (IKW active + 1KVA reactive)

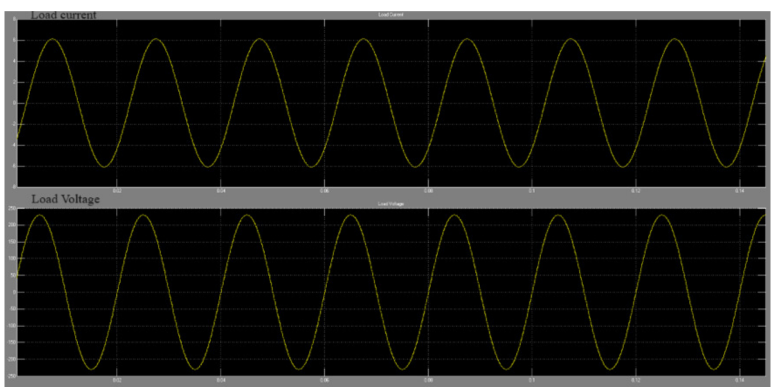

Fig 22: Load voltage and current at 1KVAR load (IKW active + 1KVA reactive parallel with IKW active + 1KVA reactive)

Table 9: Voltage and current values at PV, Wind and load end

Load	PV system		Wind System		Load parameters	
	V(V)	I(A)	V(V)	I(A)	V(V)	I(A)
1KW	137.2	3.868	137.2	2.539	230	4.35
3KW	133.2	4.734	133.2	2.641	230	13.0
5KW	143	0.002	143.0	2.106	230	21.7
6KW	131.3	0.00	131.1	3.2	230	26.0
2KVA	145.9	5.19	145.9	2.552	230	6.0

Figs 20, 21 and 22 show, 50 Hz load current and load voltage waveforms. The output voltage and current in the Photovoltaic system and wind energy system are shown in Table 9 below. Table 9 shows that the variation in the load pattern for both inductive and resistive loads. There is no change in the voltage, however, there is an increment in the load current with an increase in the load. Fig 20 shows the load current and voltage waveform for a resistive load of 1KW. The waveform shows a phasor lag of zero degrees between the voltage and current waveforms. Fig 21 shows a lag in the current phasor, as the load connected combines resistive and inductive types. Further, Fig 22 shows current and voltage waveforms with 2 strings of load combining inductive and resistive load in series. The load waveform pattern again lags with current and leads with voltage.

Thus, using MATLAB as a tool suitable voltage and current waveform patterns are studied for different load combinations, where two different energy sources are connected. However, conventionally AC bus is preferred over the DC bus to bring two or more energy forms under a single platform. The advantage of a DC bus is that it is simple and less complex. There is reduced complexity as the required voltage at the common DC bus is reached using voltage divider circuits. It has the added advantage of using a boost converter again if the required voltage level is not met.

Further, only one stage is left of converting this DC power to the required AC power, keeping the voltage at a constant value. In turn, there is a change in the load current only, which is extremely good for an efficient system.

CONCLUSION

Two independent renewable energy source-based generation schemes are modelled and simulated. When operated individually, the sources are intermittent. The two sources are combined to form a hybrid stand-alone system. The simulation results show that the intermittency is overcome and sustainable power is available. Thus, the study validates the scheme of converting flexible power to sustainable power, especially for household applications. The selection of power ratings of both schemes is justified by the load pattern of the domestic requirements. The simulation study helps develop the demonstrative models for practical applications.

REFERENCE:

[1] Sakku C. M. and Ramesh L Chakrasali, 'Comparative Analysis of Photovoltaic Characteristics Using Different Models', Journal of Electrical and Power System Engineering, 9(1), 41-52, 2023 http://matjournals.co.in/index.php/JEPSE/article/view/1781

[2] P & O algorithm link: https://in.mathworks.com/discovery/mppt-algorithm.html

[3] Vinit Kumar and Mukesh Singh, 'Derated Mode of Power Generation in PV System Using Modified Perturb and Observe MPPT Algorithm', Journal of Modern Power Systems and Clean Energy, September 2021, 9(5):1183-1192021 DOI: 10.35833/MPCE.2019.000258

[4] Ssenyimba, S., Kiggundu, N. & Banadda, 'Designing a solar and wind hybrid system for small-scale irrigation: a case study for Kalangala district in Uganda' Energy, Sustainability and Society **10**, 2020. https://doi.org/10.1186/s13705-020-0240-1

[5] Shivrath Y, Narayana PB, Thirumalasetty S and Narsaiah EL, 'Design & integration of wind-solar hybrid energy system for drip irrigation pumping application'. Int J Mod Eng Res 2(4):2947–2950, 2012. https://www.researchgate.net/publication/230669403_Design_Integration_of_Wind Solar_Hybrid_Energy_System_for_Drip_Irrigation_Pumping_Application

[6] Khan Z, Linares P and García-gonzález J, 'Integrating water and energy models for policy driven applications. A review of contemporary work and recommendations for future developments' Renew Sust Energy Reviews 67:1123– 1138, 2017 https://www.sciencedirect.com/science/article/abs/pii/S1364032116304786

[7] Bekele G and Tadesse G, 'Feasibility study of small Hydro/PV/Wind hybrid system for off-grid rural electrification in Ethiopia'. Appl Energy 97:5–15, 2012 https://ideas.repec.org/a/eee/appene/v97y2012icp5-15.html

[8] Dabra, V., Paliwal, K. K., Sharma, P., & Kumar, N, 'Optimization of the photovoltaic power system: A comparative study'. Protection and Control of Modern Power Systems, 2(1), 2017 https://pcmp.springeropen.com/articles/10.1186/s41601-017-0036-2

[9] Salman Salman, Xin Al and Zhouyang WU, 'Design of a P-&-O algorithm based MPPT charge controller for a stand-alone 200W PV system', Protection and control of Modern Power systems, 2018

[10] Yashwant Sawle, S.C. Gupta & Aashish Kumar Bohre, 'PV-wind hybrid system: A review with case study', Cogent Engineering 3: 1189305, 2016 DOI: https://doi.org/10.1080/23311916.2016.1189305

[11] Sakku C. M., Ramesh L. Chakrasali, and Nayana Shetty, 'Performance comparison of wind power generation models', Indonesian Journal of Electrical Engineering and Computer Science (under review)

[12] A. J. Mahdi, S. Fahad, and W. Tang, 'An Adaptive Current Limiting Controller for a Wireless Power Transmission System Energized by a PV Generator', Electronics, 9, 10, (2020), 1648.
https://www.mdpi.com/2079-9292/9/10/1648

[13] Shuaibu Musa Adam, Huiqing Wen, Jieming Ma, Kangshi Wang and Ka Lok Man, 'An Improved P&O MPPT Method using Boost Converter for Photovoltaic Applications', International Journal Of Design, Analysis And Tools For Integrated Circuits And Systems, Vol. 9, No. 1, November 2020
https://www.academia.edu/61661973/An_Improved_P_and_O_MPPT_Method_using_Boost_Converter_for_Photovoltaic_Applications

[14] S. Govindasamy, K. Narashiman, and R. Sasi Rama, 'High Step-Up DC-DC Converter for AC Photovoltaic Module with MPPT Control,' Journal of Electrical Engineering, vol. 65, no. 4, pp. 248-253, Aug. 2014
https://doi.org/10.2478/jee-2014-0038.

[15] O. Ibrahim, N. Z. Yahaya, N. Saad, and M. W. Umar, 'Matlab/Simulink model of solar PV array with perturb and observe MPPT for maximising PV array efficiency' in 2015 IEEE Conference on Energy Conversion (CENCON), Johor Bahru, Malaysia, 19-20 Oct. 2015: IEEE, pp. 254-258 10.1109/CENCON.2015.7409549.

[16] D. Verma, S. Nema, and R. K. Nema, 'Implementation of perturb and observe method of maximum power point tracking in Fig. 10. P&O tracking efficiency, VOL. 9, NO. 1, NOVEMBER 2020 53 SIMSCAPE/MATLAB' in 2017 International Conference on Intelligent Sustainable Systems (ICISS), Palladam, India, 7-8 Dec. 2017: IEEE, pp. 148-152
10.1109/ISS1.2017.8389387.

[17] I. Aboudrar , S. E. Hani, M. S. Heyine, and N. Naseri, 'Dynamic Modeling and Robust Control by ADRC of Grid-Connected Hybrid PV-Wind Energy Conversion System', Mathematical Problems in Engineering, Hindawi, vol.2019, pp.1-20, 2019.
https://www.hindawi.com/journals/mpe/2019/8362921/

[18] S. Datta, S. Deb, A. Datta, S. Adhikari, and B. Roy, ' Grid Connected PMSG Based Wind Energy Conversion System Using Back-to-Back Converter', Int. Conf. on Innovation in Modern Science and Technology, Springer, Cham, pp. 373-382, 2019.
https://www.researchgate.net/publication/339635151_Grid_Connected_PMSG_Based_Wind_Energy_Conversion_System_Using_Back-to-Back_Converter

[19] S. Datta, A. Islam, T. Saikia, and S. Adhikari, 'Performance study of a grid-connected permanent magnet synchronous generator-based wind turbine system', Int. Conf. on Computer, Communication, Chemical, Materials and Electronic Engineering, pp.1-4, Rajshahi, Bangladesh, 2019.
https://ieeexplore.ieee.org/document/9036566

[20] Larbi Chrifi-Alaoui, Saïd Drid , Mohammed Ouriagli and Driss Mehdi, 'Overview of Photovoltaic and Wind Electrical Power Hybrid Systems', Energies 2023, 16(12)
https://www.mdpi.com/1996-1073/16/12/4778

[21] Rashid Al Badwawi, Mohammad Abusara and Tapas Mallick, 'A Review of Hybrid Solar PV and Wind Energy System', Smart ScienceVol. 3, No. 3, pp. 127-138(2015)
https://www.tandfonline.com/doi/abs/10.1080/23080477.2015.11665647

[22] M. Engin, 'Sizing and simulation of PV-Wind hybrid power system,' International Journal of Photoenergy, 2013 1-10
https://www.hindawi.com/journals/ijp/2013/217526/

[23] P. Dalwadi, V. Shrinet, C. R. Mehta and P. Shah, 'Optimization of a solar-wind hybrid system for distributed generation,' Proc. Nirma University International Conference on Engineering (NUiCONE 11), IEEE Press, pp. 1-4, December (2011) https://www.researchgate.net/publication/261298024_Optimization_of_solar wind_hybrid_system_for_distributed_generation

[24] Z. M. Salameh and B. S. Borowy, "Optimum photovoltaic array size for a hybrid wind/PV system" IEEE Transactions on Energy Conversion, 9, 482-488 (1994) https://ieeexplore.ieee.org/document/326466